Phase Diagrams of Salt−Free Polyelectrolyte Semidilute Solutions

ARTICLE · OCTOBER 2000

DOI: 10.1021/ma000142d

Phase Diagrams of Salt-Free Polyelectrolyte Semidilute Solutions

Khaled A. Mahdi

Chemical Engineering Department, Northwestern University, Evanston, Illinois 60208

Monica Olvera de la Cruz*

Chemical Engineering Department and Material Science and Engineering Department, Northwestern University, Evanston, Illinois 60208

Received January 26, 2000; Revised Manuscript Received May 25, 2000

ABSTRACT: We analyze the phase behavior of polyelectrolyte salt-free solutions using the random phase approximation (RPA). Within this approximation, the phase diagrams of salt-free polyelectrolyte solutions show phase separation even without including short-range attractions or ion condensation. We find that the phase behavior of large chains resembles the phase diagram of polymer network solutions. That is, the equilibrium is established between a swollen network phase and a chain-free phase. Even though RPA is capable of reproducing certain aspects of the phase diagram, the model has to be modified to include ion condensation self-consistently in the analysis.

I. Introduction

Strongly charged chains in low ionic strength solutions are known to precipitate in the presence of high valence counterions.[1,2] The precipitation of the chains in the highly diluted regime is due to ion condensation. A fraction of the counterions condenses along the chain. The more compact the chain, the larger the number of condensed counterions will be, leading to neutralized dense conformations.[3] The free energy of the most compact conformation decreases linearly with the number of neutralized charges, proportional to the charge per chain N, as in an ionic glass or ionic crystal.[4] In semidilute solutions, however, the degree of ion condensation has not been determined self-consistently. Ion condensation is prominent in dilute polyelectrolyte solutions because it decreases the monopole electrostatic energy of the chains, proportional to N^2/R, where N is the number of charged monomers per chains and R is the region occupied by the chain.[5] That is, in highly dilute salt-free solutions, the free counterions do not screen the electrostatic energy because they are homogeneously mixed in the total system volume V and not within the radius of gyration of the chain R. The monopole electrostatic energy can only be reduced to $(z_m N(1 - f^c))^2/R$ if a fraction f^c of the counterions are condensed along the chains (that is, around the charged monomers) at expenses of the decrease of the entropy of mixing of the counterions. In semidilute solutions, on the other hand, unperturbed chains overlap at distances larger than ξ_e. The total charge inside the region ξ_e is zero even when the ions are free due to the electroneutrality condition. Even though the monopole electrostatic energy is zero without ion condensation,[6] ion condensation can still reduce the overall energy of the system by forming ion pairs of energy $-z_i z_m l_B/2a$, where z_i and z_m are the valences of the counterions and monomers, respectively, l_B is the Bjerrum length and $2a$ is the distance between the counterion and the monomer. However, ion condensation decreases both the screening and the favorable contribution from the thermal fluctuations of the counterions to the free energy. The self-consistent determination of the fraction of condensed counterion and the chain structure in semidilute solutions is a highly nontrivial problem.

Screening alone has been shown to be very important in molecular dynamics simulations of salt-free polyelectrolyte solutions.[7,8] Stevens and Kremer showed with simulations of both Coulombic[7] and screened[8] chains that screening and/or counterion entropy play an important and neglected role in the theory. In this paper we determine the thermodynamics of semidilute polyelectrolytes solutions assuming that the counterions are homogeneously mixed in the solution; that is, the counterions fully contribute to screen the electrostatic interactions. This approximation is known as the random phase approximation (RPA) or Debye−Hückel (DH) approximation. We emphasis that though RPA is not expected to hold in real systems because it cannot describe short-range electrostatic attractions,[2,7,8] we use RPA as a first approach to understand the effect of screening and/or counterion fluctuations in the thermodynamics.

In simple electrolyte solutions the Debye−Hückel limiting law (DHLL), which gives the well-known $-\kappa^3$ contribution to the free energy, leads to phase separation if hard core repulsions are included in the free energy.[9] There is no need to include short-range attractions between the ions to predict a salt-rich phase coexisting with a salt-poor phase. Though the DHLL overestimates the immiscibility of electrolyte solutions, it gives an approximated form for the phase diagram. Corrections to the DHLL, such as the full Debye−Hückel law (FDHL), which incorporates the diameter of the ions explicitly in solving the linearized Poisson−Boltzmann equation, underestimate slightly the critical concentration for immiscibility. Ion association further improves the Debye−Hückel approach.[9] The RPA is equivalent to the DHLL in simple electrolyte solutions. The RPA, however, allows us to introduce the chain connectivity, which in long chain solutions leads to a different electrostatic contribution to the free energy. In this paper we find that immiscibility is predicted by the free energy evaluated by RPA without the need to include short-range net monomer−monomer attractions (i.e., bad solvent effects or counterions mediated attrac-

10.1021/ma000142d CCC: $19.00
Published on Web 09/06/2000

tions), in agreement with the DHLL approach in simple electrolytes. Though the immiscibility is overestimated, the corrections to the phase diagram when ion association (referred to as ion condensation in polyelectrolyte solutions) is included in the analysis are expected to reduce the degree of immiscibility, as in the DHLL approach.

It is well-known that the DH approach and the RPA do not predict instability in simple electrolytes nor in polyelectrolytes when analyzed from the scattering function $S(k)$, calculated from the relation

$$\frac{1}{S(k \to 0)} = \frac{\partial^2 F_0}{\partial \phi^2} \tag{1}$$

where F_0 is the free energy of the electrolyte solution without fluctuations. The phase instability predicted by the DH approach in simple electrolyte solutions is due to the $-\kappa^3$ term in the free energy. This term arises from the sum of all charge fluctuations in the system. Consequently, the electrostatic contribution to the free energy must be computed to find immiscibility. In addition, the free energy is required to evaluate the coexistence curve.

There are many physical models of polyelectrolytes semidilute solutions.[2,10−14,17,18,20,22] The simplest mean field approach is due to Warren.[15] He adds to the Flory−Huggins free energy the entropy of counterions coupled with the electroneutrality condition. Here, we go further by calculating the RPA contribution to the free energy and by studying the phase behavior. Though RPA and/or modified DH approaches have been extensively used to describe charge systems,[2,13,16−18] phase diagrams have not been constructed. Most of the previous studies have analyzed the scattering function and/or the effective interactions. Though RPA is incapable of describing ion association, polyelectrolyte solutions models can use a renormalized RPA approach where the effective charge is rescaled by the condensed counterions.[2] Therefore, it is important to determine the phase behavior of this model.

In this paper, we evaluate the free energy using RPA and analyze the phase behavior without including ion condensation and/or short-range attractions. In section 2 we describe the thermodynamic approach. We find that the phase diagram resembles the phase diagram of polymer network solutions. That is, we find equilibrium between a concentrated phase and a polymer-free phase. Experiments show that indeed in the presence of multivalent ions a concentrated polyelectrolyte precipitate coexists with a dilute phase with almost no chains. The phase diagrams of salt-free polyelectrolyte solutions assumes network-solvent type phase diagrams[19] only when the number of charged segments per chain exceeds a critical value $N \sim 30$. This model predicts immiscibility for counterions of valence one and higher. The higher the valence of the counterions, the higher the temperature will be at which immiscibility occurs. Since, in our approach, we do not find self-consistently the structure−function of the chains nor do we include ion association, our results are expected to be modified when these effects are included in the concentration regimes where the chains are strongly perturbed, as discussed in the last section. In the highly dilute phase of polyelectrolytes in monovalent counterions, for example, the chains are stretched and the effective charge is strongly reduced due to ion association. Though these effects will decrease the immiscibility temperatures, they are not expected to alter the shape of the phase diagram.

II. Thermodynamic Approach

We consider a system consisting of charged chains (assumed Gaussian) and counterions (point particles) in a continuum (structureless medium). That is, the degrees of freedom of the solvent are integrated out using the incompressibility conditions. The free energy of the system is the sum of the following contributions: the ideal or entropic term of the counterions and the chains F^{id}, the hard core interactions F^{hc}, and the electrostatic term arising from charge fluctuations ΔF^e. The ideal free energy term due to the combinatorial arrangement of the particles can be expressed as

$$\frac{F^{id}}{k_B T V} = \sum_j \rho_j \ln \rho_j {\Lambda_j}^3 - \sum_j \rho_j \tag{2}$$

where ρ_j is the number density and ${\Lambda_j}^3$ is the thermal wavelength of species j. The hard core contribution indicates that the particles have a finite size and are not actually point particles. This can be expressed as

$$\frac{F^{hc}}{k_B T V} = -\sum_j \rho_j \ln (1 - \sum_j {a_j}^3 \rho_j) \tag{3}$$

where ${a_j}^3$ is the hard-core volume of species j. The monomer density is denoted by ρ_m and the counterion density by ρ_i. The counterions density is eliminated using the electroneutrality condition

$$z_m \rho_m + z_i \rho_i = 0 \tag{4}$$

where z_i is the counterion valence and z_m is the monomer valence which takes fractional value in the case of a weakly charged polyelectrolyte. The electrostatic free energy ΔF^e for simple electrolytes can be obtained from the Debye−Hückel theory, or an equivalent, nevertheless, more general method, such as RPA.[11,17] The RPA, also known as the Gaussian approximation, characterizes the fluctuations of the system. Here, we give the final results of RPA without the explicit details that are explained elsewhere.[13,23] In polymer physics the RPA was first proposed by Edwards.[24] He constructed the free energy in terms of $\hat{\rho}(\mathbf{k})$, the Fourier transform of the local number density, as

$$e^{-(F-F_0)/kT} = \int e^{-U[\hat{\rho}(\mathbf{k})]/k_B T} \prod_{\mathbf{k}>0} d\hat{\rho}(\mathbf{k}) \tag{5}$$

where $U[\hat{\rho}(\mathbf{k})]$ is the system energy expressed in term of the density fluctuations. The energy $U[\hat{\rho}(\mathbf{k})]$ for a single component is expressed as

$$\frac{U[\hat{\rho}(\mathbf{k})]}{k_B T} = V \sum_{\mathbf{k}>0} \hat{\rho}(\mathbf{k}) \hat{A}(\mathbf{k}) \hat{\rho}(-\mathbf{k}) \tag{6}$$

where $\hat{A}(\mathbf{k})$ is the inverse of the structure−function defined as $\hat{G} = V\langle \hat{\rho}(\mathbf{k}) \hat{\rho}(-\mathbf{k}) \rangle$; the average is over the distribution function given by $(1/Z)e^{-U[\hat{\rho}(\mathbf{k})]/kT}$, where Z is the partition function. Since the higher order terms in eq 6 are neglected, the validity of RPA is restricted to systems that exhibit low density fluctuations. Ex-

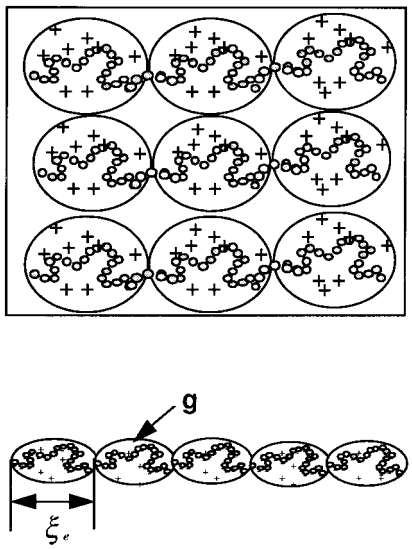

Figure 1. Scheme of a semidilute polyelectrolyte solution showing the electrostatic blobs.

amples include concentrated polymer solutions and semidilute polyelectrolyte solutions. The validity of RPA to describe semidilute polyelectrolyte solutions is addressed in the next section. Equation 6 can easily be extended to include several components. Instead of $\hat{\rho}(\mathbf{k})$, which represents one component, we use vector representation to accommodate all the components of the system $\hat{\rho}_i(\mathbf{k})$. $\hat{A}(\mathbf{k})$ becomes a $n \times n$ matrix with $\hat{A}_{ij}(\mathbf{k})$ elements. We use tensorial notation to represent matrices

$$\frac{U[\{\hat{\rho}_i(\mathbf{k})\}]}{k_B T} = V \sum_{\mathbf{k}>0} \sum_{ij} \hat{\rho}_i(\mathbf{k})\, \hat{A}_{ij}(\mathbf{k})\, \hat{\rho}_j^{\dagger}(-\mathbf{k}) \qquad (7)$$

where the dagger represents the transpose. Next, we evaluate the free energy of the system by substituting eq 7 into eq 5 and by performing the integration over all components and wave vectors. The resultant free energy expression takes the form

$$\frac{\Delta F}{k_B T\, V} = \frac{1}{2(2\pi)^3} \int \ln\left[\frac{\det[\hat{A}_{ij}(\mathbf{k})]}{\det[\hat{A}_{ij}{}^{0}(\mathbf{k})]}\right] d\boldsymbol{k} \qquad (8)$$

where $\hat{A}_{ij}{}^{0}(\mathbf{k})$ represents the reference state, usually taken as the state of no interactions. On the basis of this equation, we evaluate the free energy contribution due to charge fluctuations. The major drawback of RPA is the divergence of the final integral, eq 8. The divergence is mainly attributed to the self-energy term, which has to be subtracted properly.

A. Random Phase Approximation Free Energy of Polyelectrolyte Solutions. As mentioned above, RPA is applicable to systems with small concentration fluctuations. In the case of polyelectrolyte solutions, the concentration fluctuations are low when the electrostatic interactions are weak and almost independent of the local properties of the chain. To justify this assumption, we develop the following scaling argument. The semidilute solution can be described as a homogeneous collection of electrostatic blobs with counterions inside the blobs. According to our electrostatic blob picture, shown in Figure 1, the chain is subdivided into blobs each of size ξ_e that contains g monomers. Within the blob, there are counterions of valence z_i. The monopole electrostatic energy per blob is given by

$$F^{e}_{blob} = \sum_{\alpha,\beta} \int d\mathbf{r} \int d\mathbf{r}' \rho_\alpha(\mathbf{r}) \rho_\beta(\mathbf{r}')\, u_{\alpha\beta}(|\,\mathbf{r} - \mathbf{r}'|) \qquad (9)$$

where $u_{\alpha\beta}$ is the electrostatic energy between species α and β, for instance monomer and counterion. Electrostatic blob models generally exclude the counterions in the blob when analyzing semidilute solution.[17,20] If one ignores the counterions, one obtains the result, $F^{e}_{blob}/k_B T \sim l_B z_m{}^2 g^2/\xi_e$. If the electrostatic energy per thermal energy is much greater than one, the chain inside the blob is stretched, which is true at infinite dilution. In highly dilute salt-free solutions, the counterions can be ignored because the chains do not overlap ($g = N$ and $\xi_e = R_g$), so there are not enough counterions inside the blob to allow charge cancellation (the entropy of the counterions in the whole system volume dominates). However, the counterions are essential in the blob picture in semidilute solutions because the chains overlap and the solution is electrically neutral. In this case, the above electrostatic energy is identically zero when densities are assumed spatially invariant. The effective electrostatic energy between the monomers in the presence of fluctuating counterions can be estimated by integrating out the counterions. This results in a screened potential given by $u_{mm} \sim z_m{}^2 e^{-\kappa_i r}/r$ where κ_i is Debye's inverse screening length defined as $\kappa_i{}^2 = 4\pi l_B z_i{}^2 \rho_i$ with $\rho_i = |z_m/z_i|\rho_m$. Assuming constant monomer density inside a blob of size ξ_e, eq 9—after substituting the screened potential—becomes

$$F^{e}_{blob} \sim k_B T l_B \frac{z_m{}^2 g^2}{\xi_e{}^3}\left(\frac{1}{\kappa_i{}^2} - \frac{e^{-\kappa_i \xi_e}}{\kappa_i{}^2}(1 + \kappa_i \xi_e)\right) \qquad (10)$$

RPA is applicable when the effective monomer−monomer electrostatic energy is of the order of the thermal energy, i.e., $F^{e}_{blob} \sim k_B T$. In semidilute solutions of weakly charged chains, $\kappa_i \xi_e < 1$, eq 10 reduces to $F^{e}_{blob}/k_B T \sim l_B z_m{}^2 g^2/\xi_e$. Therefore, the monopole electrostatic energy is of the order of the thermal energy at length scales less than $\xi_e = l_B z_m{}^2 g^2$, where $g = (\xi_e/a)^2$, leading to $\xi_e = a^{4/3}/(l_B{}^{1/3} z_m{}^{2/3})$. The mesh size ξ_m (the size at which the chains overlap) if Gaussian statistics are obeyed at all length scales bigger than the monomers size a, is given by $\xi_m = 1/(a^2 \rho_m)$. In weakly charged chains Gaussian statistics are obeyed when ξ_m is smaller than the electrostatic blob,[6,17,20,22] ξ_e, that is, when the monomer concentration $\rho_m > l_B{}^{1/3} z_m{}^{2/3}/a^{10/3}$.

Semidilute solutions of strongly charged chains, $\kappa_i \xi_e > 1$, are complicated. In this limit eq 10 reduces to

$$F^{e}_{blob} \sim k_B T \frac{l_B}{(\xi_e \kappa_i)^2} \frac{z_m{}^2 g^2}{\xi_e} \qquad (11)$$

That is, the monopole electrostatic energy is reduced by $1/(\xi_e \kappa_i)^2$ due to the screening of the counterions. Since most scaling theories ignore screening, this factor is missing; they instead obtain $F^{e}_{blob}/k_B T \sim l_B z_m{}^2 g^2/\xi_e > 1$. Therefore, it is common in scaling models to assume that in this case the counterions will condense along the chain, as in the Manning model, to reduce its effective charge and recover the weakly charged chains result discussed above. The fraction of condensed counterions, however, has to be determined self-consistently by computing the strong correlations between the ions

and the monomers,[21] ignored in the Manning model. Recently Schiessel[22] attempted to add some of the corrections to the Manning model by assuming that ion condensation leads to weak attractions due to fluctuating dipole-charge and fluctuating dipole−dipole interactions. As discussed in the Introduction, in this paper we do not attempt to find the fractions of condensed counterions. We aim to determine the effects of screening in the phase diagram assuming all of the counterions are free. In this approximation Gaussian statistics will be obeyed when

$$\frac{z_m{}^2 l_B g^2}{(\xi_e \kappa_i)^2 \xi_e} \sim 1 \tag{12}$$

The Gaussian mesh size is smaller than ξ_e if the concentration $\rho_m \gg \rho_m^*$, where

$$\rho_m^* \sim \frac{1}{a^3}\left(4\pi\left|\frac{z_i}{z_m}\right|\right)^{-1/2} \tag{13}$$

Therefore, if we assume all of the counterions are homogeneously free, RPA in strongly charged chains is applicable only at high concentrations. This is expected given that in this approximation screening reduced the elelctrostatic energy to an excluded volume type potential inside the blob, $v\ g^2/\xi_e{}^3$ with $v = l_B\ z_m{}^2/\kappa_i{}^2$ as suggested by eq 11. For simplicity, the electrostatic blobs are assumed to obey Gaussian statistics, even when we are analyzing polyelectrolyte solutions in good solvents, and $\rho < \rho_m^*$.

In the remainder of this paper, we compute the phase diagram of a system of overlapping ideal polyelectrolyte chains with free point counterions in a continuum (i.e., the solvent). The structure−function of a Gaussian chain is often approximated within 15% error to[24]

$$\hat{G}_{mm}(\mathbf{k}) = \frac{N\rho_m}{1 + (1/2)R_g{}^2 k^2} \tag{14}$$

where $R_g{}^2$ is the square of the radius of gyration given by $(1/6)a^2N$ and N is the number of monomers. The point counterion structure−function equals its mean density ρ_i (one can deduce it from eq 14 by setting $N = 1$ and $R_g = 0$). There are no cross terms in density because the interactions between the monomers and counterions are mainly electrostatic and will appear in the interaction matrix only. Therefore, the neutral correlation matrix $\hat{A}_{ij}^0(\mathbf{k})$ (the inverse of the structure matrix) has two components defined as

$$\hat{A}_{11}^0(\mathbf{k}) = \frac{1}{\hat{G}_{mm}(\mathbf{k})} \tag{15}$$

$$\hat{A}_{22}^0(\mathbf{k}) = \frac{1}{\rho_i} \tag{16}$$

The system matrix, $\hat{A}_{ij}(\mathbf{k})$ is the sum of neutral $\hat{A}_{ij}^0(\mathbf{k})$ and electrostatic $\hat{A}_{ij}^e(\mathbf{k})$ parts. The electrostatic contribution is found from the Coulombic potential[25] between the charges, in our case the monomers and counterions

$$\frac{U^e(|\mathbf{R}_i - \mathbf{R}_j|)}{k_B T} = \frac{1}{2}\sum_{i\neq j} l_B \frac{z_i z_j}{|\mathbf{R}_i - \mathbf{R}_j|} \tag{17}$$

Representing eq 17 in terms of $\hat{\rho}(\mathbf{k})$

$$\frac{U^e[\{\hat{\rho}_i(\mathbf{k})\}]}{k_B T} = 4\pi l_B V \sum_{\mathbf{k}>0}\sum_{ij}\hat{\rho}_i(\mathbf{k})\frac{z_i z_j}{k^2}\hat{\rho}_j^{\dagger}(-\mathbf{k}) \tag{18}$$

By comparing eq 18 to eq 7, we identify $\hat{A}_{ij}^e(\mathbf{k})$ as $4\pi l_B z_i z_j/k^2$ and

$$\hat{A}_{ij}(\mathbf{k}) = \hat{A}_{ij}^0(\mathbf{k}) + 4\pi l_B \frac{z_i z_j}{k^2}$$

Substituting $\hat{A}_{ij}(\mathbf{k})$ and $\hat{A}_{ij}^0(\mathbf{k})$ into eq 8, we obtain the RPA contribution to the free energy,

$$\frac{\Delta F^e}{k_B T\ V} = \frac{1}{2(2\pi)^3}\int \ln\left[1 + \frac{\kappa_i{}^2}{k^2} + \frac{N\kappa_m{}^2}{k^2(1 + s^2k^2)}\right] - \frac{\kappa_i{}^2}{k^2} - \frac{N\kappa_m{}^2}{k^2(1 + s^2k^2)}\,\mathrm{d}\mathbf{k} \tag{19}$$

where $\kappa_m{}^2 = 4\pi l_B z_m{}^2 \rho_m$ and $\kappa_i{}^2 = 4\pi l_B z_i{}^2 \rho_i$ are the ionic strength of the monomers and free counterions, respectively, and $s^2 = (1/2)R_g{}^2 = (1/12)a^2N$. The last terms are subtracted from the logarithmic term only to avoid the need of a cutoff in the integral due to its divergence at long k values. These terms do not contribute to the thermodynamics because they are linear in the polymer concentration (when one includes ion condensation, since κ_i is a function of the fraction of condensed counterions, this subtraction is not allowed; this is a serious mistake in the free energy computed in ref 2). Notice that only the term proportional to $\kappa_i{}^2/k^2$ is necessary because there is no divergence in the large k limit in the integral of the logarithmic term from the charged monomers. Indeed, the chain connectivity gives a much faster decay than $1/k^2$ for the electrostatic interactions at short wavelengths; this is also true for Gaussian chains made of blobs which monomers obey self-avoiding walk statistics. The irrelevant subtracted term proportional to $N\kappa_m{}^2$ only facilitates the algebra and gives an electrostatic contribution that reduces to the simple Debye−Hückel electrostatic free energy in the correct limit, discussed below. The final electrostatic free energy is

$$\frac{\Delta F^e}{k_B T\ V} = \frac{-1}{48\pi s^3}[\sqrt{2}\,(X - Y)^{3/2} + \sqrt{2}\,(X + Y)^{3/2} + 6s^2\kappa_m{}^2 - 4] \tag{20}$$

where X and Y are given by the following equations:

$$X = 1 + s^2\kappa_i{}^2 \tag{21}$$

$$Y^2 = (1 - s^2\kappa_i{}^2)^2 - 4s^2N\kappa_m{}^2 \tag{22}$$

Equation 20 does reduce to $-(\kappa_i{}^2 + \kappa_m{}^2)^{3/2}/12\pi$, the simple Debye−Hückel electrostatic free energy, if the radius of gyration of the polymer approaches 0 and the number of monomers N is set to 1. Other expressions for the electrostatic free energy of the same system reported in the literature do not converge to the Debye−Hückel theory at the prescribed limit.[2,17] To recover the infinite chain limit, we first substitute the value of $s^2 = a^2N/12$, then we take the limit $N \to \infty$. The electrostatic free energy will be exactly the same as if we

started with an infinite chain with the structure−function given by $12/(ak)^2$. The infinite-chain electrostatic free energy becomes

$$\frac{\Delta F^{e}}{k_B T\, V} = \frac{-1}{48\pi}[\sqrt{2}(\kappa_i^{\,2} - \sqrt{\kappa_i^{\,4} - 48(\kappa_m^{\,2}/a^2)})^{3/2} + \sqrt{2}(\kappa_i^{\,4} - \sqrt{\kappa_i^{\,4} - 48(\kappa_m^{\,2}/a^2)})^{3/2}] \quad (23)$$

In the case of low monomer density eq 23 reduces to the $(k_m/a)^{3/2}/(3^{1/4}\pi)$, as obtained in refs 2 and 17.

B. Total Free Energy and Phase Diagrams. The total free energy of the system is the sum of entropic, hard core, and electrostatic contributions found in eq 20

$$\frac{\Delta F}{k_B T} = \left(\frac{1}{N} - \frac{z_m}{z_i}\right)\phi_m[\ln \phi_m - \ln(1-\phi_m)] - \frac{(X^* + Y^*)^{3/2}}{24\sqrt{2}\pi} - \frac{(X^* - Y^*)^{3/2}}{24\sqrt{2}\pi} \quad (24)$$

where $\phi_m = \rho_m a^3$, X^* and Y^* are defined as follows after substituting for κ_i and κ_m

$$X^* = \frac{12}{N} + 4\pi\xi|z_i z_m|\phi_m \quad (25)$$

$$Y^* = \sqrt{\left(\frac{12}{N} - 4\pi\xi\left|z_i z_m\right|\phi_m\right)^2 - 192\pi\xi z_m^{\,2}\phi_m} \quad (26)$$

where $\xi = l_B/a$ is the dimensionless Bjerrum length. Notice that ξ is the "energy" parameter in the free energy over $k_B T$. The coexistence curve is calculated by equating the chemical potential and the pressure of the system at a fixed value of ξ, which is equivalent to constant temperature.

$$P^\alpha = P^\beta = P_{eq} \quad (27)$$

$$\mu^\alpha = \mu^\beta = \mu_{eq} \quad (28)$$

Instead of solving the highly nonlinear algebraic equations simultaneously (notice the complexity of the free energy), we find the equilibrium pressure and equilibrium chemical potential. A plot of the pressure against the chemical potential will intersect itself if two phases coexist in the system. The intersection point is the equilibrium point.[26] The instability curve or spinodal is determined from the criterion of critical behavior, mathematically expressed as the second derivative of the free energy set equal to zero

$$\frac{\partial^2 F}{\partial \phi^2} = 0 \quad (29)$$

Figure 2 shows the phase diagram of polyelectrolyte solutions at large N with $z_i = 3$. The curve illustrates two branches. The first branch is at $\phi_m \sim 0$, the other branch indicates a very concentrated phase at around $\phi_m \sim 0.8-0.9$. The spinodal and the binodal touch each other at the critical point $\xi^{cr} \sim 0.20$. Figure 3 illustrates the coexistence curves at different counterion valences. The higher the valence, for instance at $z_i = 4$, the more concentrated the polymer-rich phase will be at lower ξ value. The critical point ξ^{cr}, at different valences, is found to obey the following relation

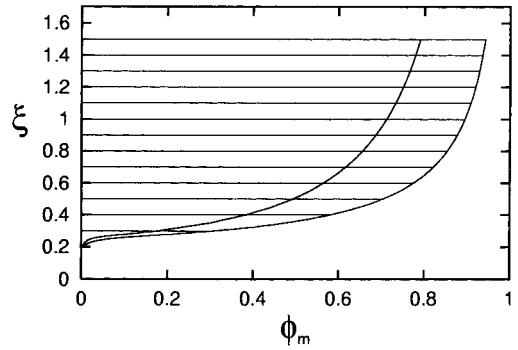

Figure 2. Phase diagram (binodal and spinodal) of a fully charged polyelectrolyte with counterions of valence $z_i = 3$.

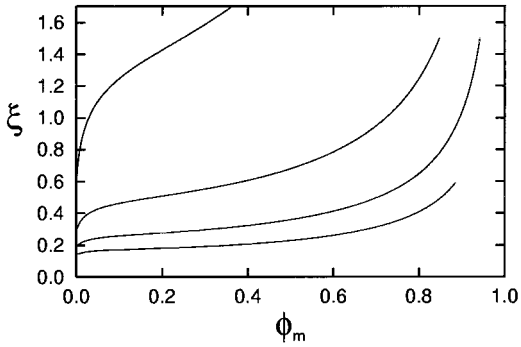

Figure 3. Effect of the counterion valence $z_i = 1$, 2, 3, 4 on phase diagrams for fully charged polyelectrolytes ($z_i = 1$ is the top curve and $z_i = 4$ is the lowest curve) as predicted by the model.

$$\xi^{cr} = \frac{3/5}{|z_m z_i|} \quad (30)$$

Figure 4 shows plots of the phase behavior at different values of chain segments N. The figure demonstrates the effect of connectivity on the phase diagram. We found that there exists a value of N, above which the system's phase diagram exhibits an inflection point. This value is estimated numerically at about $N^* \sim 30$. For N values lower than N^*, the spinodal has the usual "U" shape, similar to simple electrolyte solutions. Above N^*, the phase diagram assumes an "S" shape that resembles a polymer network solution. In uncharged swollen polymer networks, the strain energy generated by the cross-links leads to the coexistence of a swollen network phase and a phase with no chains. The infinite chain connectivity in networks is responsible for the "S" shape phase diagram.

III. Discussion and Conclusions

In RPA, phase separation in salt-free polyelectrolyte solutions results from the electrostatic contribution to the free energy. That is, short-range attractions are not necessary to predict immiscibility, suggesting that polyelectrolytes precipitate even in good solvent conditions. Indeed, the salt-free phase diagrams shown here indicate immiscibility for all valences of the counterions at sufficiently low ξ (high l_B/a) values. Experiments show immiscibility only at valences higher than 3 in polyelectrolytes with fixed structural charges, such as PSS and single stranded DNA. If we add short-range attraction to the system to represent the hydrophobic nature of the monomers, we expect immiscibility even at lower ξ values. This suggests that polyelectrolytes with monovalent counterions are not water-soluble, in disagreement

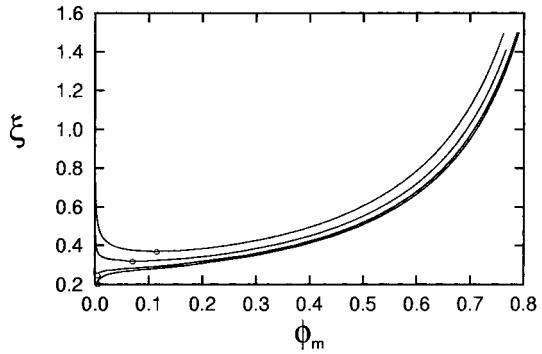

Figure 4. Phase diagrams of polyelectrolyte solutions at different value of N. The top value corresponds to $N = 10$ and the bottom value is for the infinite chain. The plots show a critical value above which the systems show inflection points at approximately $N^* \sim 30$. The curves are spinodals (the same behavior is exhibited by the binodals).

with the experimental observations. The model, therefore, underestimates the value of ξ at which immiscibility starts. The same problem was observed by Fisher and Levin[9] in the case of simple electrolyte solution. These authors suggested the use of the full DH expression for the free energy, which underestimates the physical phase behavior. To solve that problem, they introduced ion association and the resulting dipole−dipole attractions of the neutralized ion pairs.

We have incorporated into the RPA the hard-core volume of the ions on the electrostatic free energy. Unfortunately, the effect of the hard-core volume is found to be minimal on the phase diagram. One way of improving the present RPA phase diagram is assuming that a fraction of the counterions condense to form electrically neutral bonds. In the case of monovalent counterions ion association decreases the immiscibility and increases the value of N at which a networklike phase diagram is predicted by RPA, as expected. However, if the counterions are multivalent, these bonds lead to bridges between chains, forming a polymer network. The network like phase diagram predicted here appears as soon as the electrostatic energy gain of associating z_i monomers of valence −1 with one multivalent ion of valence z_i is greater than the thermal energy, $z_i^2\xi > 1$, increasing the immiscibility. A phase diagram including these effects will be published elsewhere.[27]

Another issue that needs to be addressed is that the poor−polymer phase, predicted by RPA, is usually in the highly dilute regime where the model is not applicable. The chains in the dilute regime have a different structure−function. The correct free energy of the dilute phase must be constructed. Recent scaling theories have emerged to describe the chain conformation of polyelectrolyte dilute solutions,[28] which should help to estimate the free energy of the dilute solution.

At present, there is no self-consistent model that describes the phase diagram of polyelectrolytes. In refs 1 and 2, the electrostatic RPA contribution to the spinodal was neglected and it seems to give reasonable results. In these and in other models,[3,28] the existence of short-range attractions to predict the precipitation of polyelectrolytes is essential. Only recently, chain precipitation in dilute solutions from extended to dense conformations was predicted by including only charge fluctuations and hard core monomer−monomer repulsions in the free energy of a finite system of size R_g. However, in this study,[16] Brilliantov et al. ignore the chain connectivity. Including only the charge fluctuations of the counterions inside the dense chain, they found a transition to a dense structure at extremely large ξ values, at which there should be no charge fluctuations.[4] In semidilute solutions, on the other hand, including chain connectivity we find precipitation at much lower values of ξ. We find immiscibility in the presence of monovalent counterions even at $\xi < 1$, suggesting that ion condensation may be important also in weakly charged chains.

References and Notes

(1) Raspaud, E.; Olvera de la Cruz, M.; Sikorav, J. L.; Livolant, F. *Biophys. J.* **1998**, *74*, 381.
(2) Olvera de la Cruz, M.; Belloni, L.; Delsanti, M.; Dalbiez, J. P.; Spalla, O.; Drifford, M. *J. Chem. Phys.* **1995**, *103*, 5781.
(3) Gonzalez-Mozuelos, P.; Olvera de la Cruz, M. *J. Chem. Phys.* **1995**, *103*, 3145.
(4) Solis, F. J.; Olvera de la Cruz, M. *J. Chem. Phys.* **1999**, *112*, 2030.
(5) de Gennes, P. G.; Pincus, P.; Velasco, R. M.; Brouchard, F. *J. Phys. II (Fr.)* **1976**, *37*, 1461.
(6) Barrat, J.-L.; Joanny, J.-F. *Adv. Chem. Phys.* **1996**, *94*, 17.
(7) Stevens, M.; Kremer, K. *J. Chem. Phys.* **1995**, *103*, 1669.
(8) Stevens, M.; Kremer, K. *J. Phys. II Fr.* **1996**, *6*, 1607.
(9) Fisher, M. E.; Levin, Y. *Phys. Rev. Lett.* **1993**, *71*, 3826.
(10) Borukhov, I.; Andelman, D.; Orland, H. *Eur. Phys. J. B* **1998**, *5*, 869.
(11) Joanny, J. F.; Leibler, L. *J. Phys. Fr.* **1990**, *51*, 545.
(12) Jiang, J.; Liu, H.; Hu, Y.; Prausnitz, J. M. *J. Chem. Phys.* **1998**, *108*, 780.
(13) Vilgis, T. A.; Borsali, R. *Phys. Rev. A* **1991**, *43*, 6857.
(14) Muthukumar, M. *J. Chem. Phys.* **1996**, *105*, 5183.
(15) Warren, P. B. *J. Phys. II Fr.* **1997**, *7*, 343.
(16) Brilliantov, N. V.; Kuznetsov, D. V.; Klein, R. *Phys. Rev. Lett.* **1998**, *81*, 1433.
(17) Borue, V. Y.; Erukhimovich, I. Y. *Macromolecules* **1988**, *21*, 3240.
(18) Donley, J. P.; Rudnick, J.; Liu, A. J. *Macromolecules* **1997**, *30*, 1188.
(19) Bauer, B. J.; Briber, R. M.; Han, C. C. *Macromolecules* **1989**, *22*, 940.
(20) Dobrynin, A. V.; Rubinstein, M. *Macromolecules* **1999**, *32*, 915.
(21) Solis, F. J.; Olvera de la Cruz, M. *Phys. Rev. E* **1999**, *60*, 4496.
(22) Schiessel, H. *Macromolecules* **1999**, *32*, 5673.
(23) Olvera de la Cruz, M.; Edwards, S. F.; Sanchez, I. C. *J. Chem. Phys.* **1988**, *89*, 1704.
(24) Doi, M.; Edwards, S. F. *The Theory of Polymer Dynamics*; Clarendon Press: Oxford, England, 1986.
(25) McQuarrie, D. A. *Statistical Mechanics*; Harper and Row: New York, 1976.
(26) Callen, H. *Thermodynamics and An Introduction to Thermostatistics*, 2nd ed.; Wiley: New York, 1985.
(27) Mahdi, K. A.; Olvera de la Cruz, M. Manuscript in preparation.
(28) Schiessel, H.; Pincus, P. *Macromolecules* **1998**, *21*, 7953.

MA000142D